Revista de Ciencias Tecnológicas (RECIT). Universidad Autónoma de Baja California ISSN 2594-1925
Volumen 9 (3): e498. Julio-Septiembre, 2026. https://doi.org/10.37636/recit.v9n3e498

Research article

Development of a machining allowance model for rectangular pocket milling operations

Desarrollo de un modelo de tolerancia de mecanizado para operaciones de fresado de cavidades rectangulares

Tran Thanh Tung[1], Nguyen Thi Anh[2], Nguyen Xuan Quynh[3], Tran Vu Minh[3,*]

[1]Faculty of Engineering Mechanics and Automation, VNU University of Engineering and Technology, Hanoi, Vietnam
[2]Faculty of Mechanical Engineering, Thuyloi University, Hanoi, Vietnam
[3]School of Mechanical Engineering, Ha Noi University of Science and Technology, Hanoi, Vietnam

[*]**Corresponding author:** Tran Vu Minh, School of Mechanical Engineering, Ha Noi University of Science and Technology, Hanoi, Vietnam. E-mail: minh.tranvu@hust.edu.vn ORCID: 0000-0003-0621-9217.

Received: June 12, 2026 **Accepted:** June 23, 2026 **Published:** July 8, 2026

Abstract.- *Machining allowance plays a critical role in determining productivity, energy consumption, cutting force, and dimensional accuracy in pocket milling operations, yet it is commonly selected empirically in industrial practice. This study proposes an analytical, optimization-based framework for determining an efficient machining allowance for rectangular pocket milling. Mathematical models are developed to quantify total energy consumption, machining time, and peripheral cutting force as functions of cutting parameters and allowance distribution between rough and finish milling stages. A multi-objective optimization problem is formulated and solved using the Non-dominated Sorting Genetic Algorithm II (NSGA-II) to simultaneously minimize energy consumption, machining time, and cutting force. Experimental validation is conducted on polymer workpieces and compared with CAM-recommended parameters. The results show that the balanced Pareto-optimal solution reduces machining time from 5 min 58.52 s to 2 min 26.47 s, corresponding to an approximate 59% reduction, and decreases the peripheral cutting force from 698.18 N to 382.73 N, corresponding to an approximate 45% reduction, while achieving the target pocket depth of approximately 22 mm and eliminating the ~2 mm over-machining observed under CAM-default settings. A minimum-energy solution further reduces energy consumption from 0.44 kWh to 0.267 kWh, but at the cost of a significantly increased cutting force (1203.45 N). These results indicate that treating machining allowance as an optimization variable enables systematic trade-offs among productivity, energy consumption, cutting force, and dimensional accuracy, offering a practical alternative to conventional CAM-based parameter selection.*

Keywords: Machining allowance; Pocket milling; Multi-objective optimization; Energy consumption; Cutting force.

Resumen. - El margen de mecanizado desempeña un papel fundamental en la determinación de la productividad, el consumo de energía, la fuerza de corte y la precisión dimensional en las operaciones de fresado de cavidades; sin embargo, en la práctica industrial, suele seleccionarse de forma empírica. Este estudio propone un marco analítico y de optimización para determinar un margen de mecanizado eficiente en el fresado de cavidades rectangulares. Se desarrollan modelos matemáticos para cuantificar el consumo total de energía, el tiempo de mecanizado y la fuerza de corte periférica en función de los parámetros de corte y la distribución del margen entre las etapas de fresado de desbaste y acabado. Se formula y resuelve un problema de optimización multiobjetivo mediante el algoritmo genético de clasificación no dominada II (NSGA-II) para minimizar simultáneamente el consumo de energía, el tiempo de mecanizado y la fuerza de corte. Se realiza una validación experimental en piezas de polímero y se compara con los parámetros recomendados por CAM. Los resultados muestran que la solución óptima de Pareto equilibrada reduce el tiempo de mecanizado de 5 min 58,52 s a 2 min 26,47 s (lo que corresponde a una reducción aproximada del 59 %) y disminuye la fuerza de corte periférica de 698,18 N a 382,73 N (lo que corresponde a una reducción aproximada del 45 %), al tiempo que alcanza la profundidad de cavidad objetivo de aproximadamente 22 mm y elimina el sobremecanizado de ~2 mm observado con la configuración predeterminada de CAM. Una solución de energía mínima reduce aún más el consumo de energía de 0,44 kWh a 0,267 kWh, pero a costa de un aumento significativo de la fuerza de corte (1203,45 N). Estos resultados indican que tratar el margen de mecanizado como una variable de optimización permite realizar compensaciones sistemáticas entre productividad, consumo de energía, fuerza de corte y precisión dimensional, ofreciendo una alternativa práctica a la selección de parámetros convencional basada en CAM.

Palabras clave: Margen de mecanizado; Fresado de cavidades; Optimización multiobjetivo; Consumo de energía; Fuerza de corte.

ISSN: 2594-1925

1. Introduction

Machining operations are commonly performed through a sequence of roughing and finishing stages in order to balance productivity and dimensional accuracy [1-5]. During rough machining, large amounts of material are removed at high material removal rates, often at the expense of geometric accuracy and surface integrity. To ensure that the final component meets design specifications, a certain amount of material, referred to as machining allowance or excess material, is intentionally left on the workpiece after rough machining and subsequently removed during the finishing stage.

Machining allowance plays a critical role in determining the overall performance of the machining process [6-9]. As schematically illustrated in Figure 1, machining allowance represents the intermediate material layer between the rough-machined surface and the final finished surface. This allowance must be sufficient to compensate for surface irregularities, elastic deformation of the tool–workpiece–fixture system, tool runout, and positioning errors generated during rough machining. At the same time, excessive allowance during finishing leads to increased cutting forces, accelerated tool wear, higher energy consumption, and increased vibration, which may deteriorate surface quality and reduce machining stability.

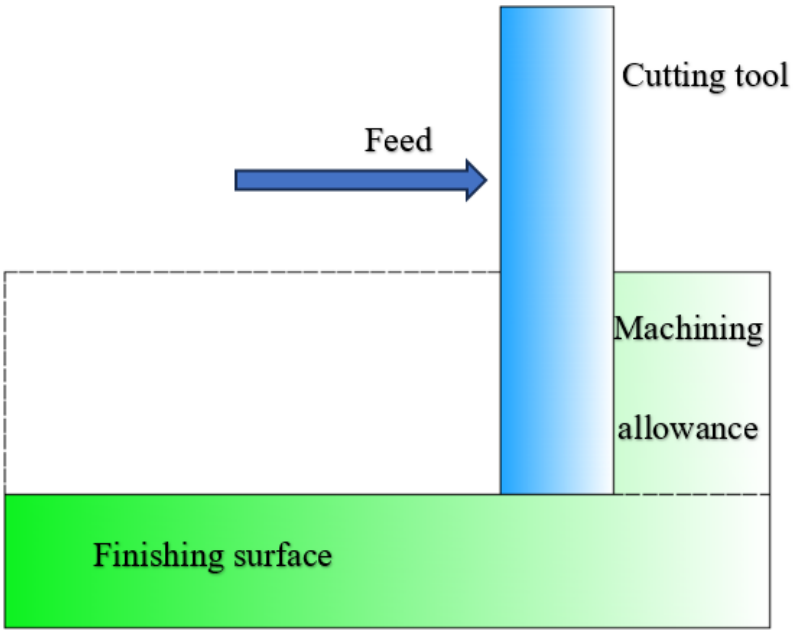

Figure 1. Machining allowance removal in milling during the finishing stage.

Pocket milling is one of the most fundamental and widely used machining operations in modern manufacturing, particularly in the production of molds, dies, structural components, and mechanical parts with internal cavities [10-12]. Owing to its flexibility and high material removal capability, CNC pocket milling is extensively applied in aerospace, automotive, and general mechanical industries. However, despite its apparent simplicity, achieving both high productivity and stable machining quality remains challenging. The pocket milling process involves complex interactions among cutting parameters, tool geometry, material properties, and machine tool dynamics, which become especially pronounced during multi-stage machining operations.

To illustrate the geometric characteristics of pocket milling and the relationship between rough and finish machining stages, a schematic of a typical rectangular cavity milling process is shown in Figure 2. The figure highlights the finishing surface and the remaining machining allowance after rough

ISSN: 2594-1925

milling, which plays a critical role in determining cutting stability, surface integrity, and dimensional accuracy during the finishing stage.

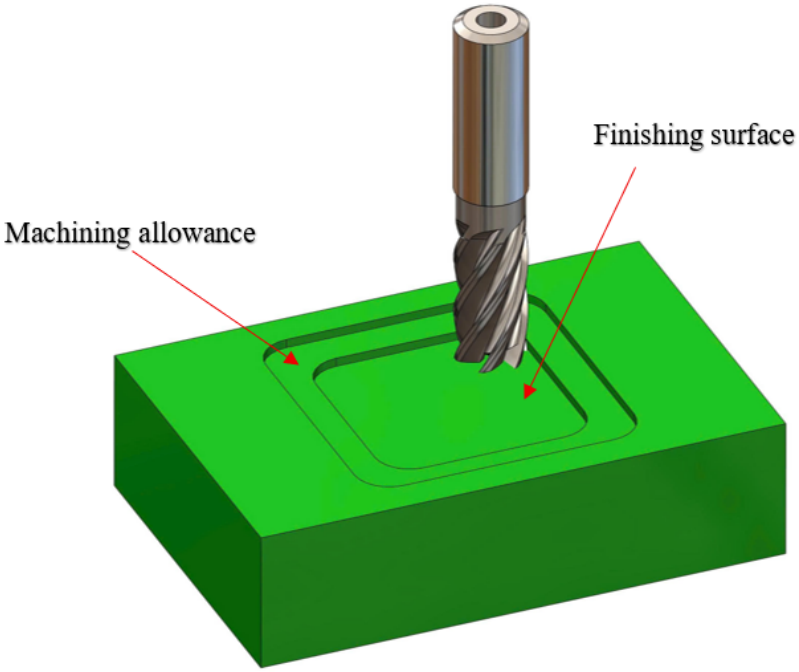

Figure 2. Rectangular cavity milling and definition of machining allowance.

In industrial practice, machining allowance is often determined empirically based on operator experience or general machining guidelines. However, such experience-based selection does not account for the complex and nonlinear relationships between allowance, cutting parameters, and machining performance. An improper allocation of machining allowance can lead to several undesirable consequences. Excessive remaining allowance increases the cutting load during the finishing stage, resulting in elevated cutting forces, accelerated tool wear, higher energy consumption, and increased machine vibration. Conversely, insufficient allowance after rough milling limits the ability of the finishing process to correct geometric errors and surface irregularities, thereby preventing the achievement of the required dimensional accuracy and surface roughness. These issues are particularly critical in the milling of pockets with sharp corners or rectangular geometries, where tool engagement conditions vary significantly along the toolpath.

Previous studies on milling have primarily focused on cutting force modeling, toolpath optimization, chatter stability, and surface quality prediction [13-20]. While these studies have contributed significantly to the understanding of milling mechanics, machining allowance is often treated as a fixed or predefined parameter rather than a decision variable to be optimized. Only limited research has attempted to establish a quantitative relationship between machining allowance, machining time, and quality constraints, especially for rectangular pocket geometries commonly encountered in practical manufacturing. As a result, process planners still lack a systematic and scientific method for determining an efficient machining allowance that balances productivity, energy efficiency, cutting load, and quality requirements.

To address this research gap, this study proposes a mathematical and optimization-based model for determining an efficient machining allowance in rectangular pocket milling operations, with particular emphasis on rectangular pockets. The proposed model establishes analytical relationships between machining allowance, toolpath characteristics, cutting parameters, machining time, *energy* consumption, cutting force, and dimensional accuracy. Based on these relationships, a multi-objective

ISSN: 2594-1925

optimization framework is formulated to determine the optimal allocation of machining allowance between roughing and finishing stages. The objectives are to minimize total machining time while satisfying constraints related to surface roughness and dimensional accuracy.

2. Materials and methods

2.1. Energy, Machining Time, and Cutting Force Models

The analytical formulations adopted in this study are based on established energy, time, and cutting force models reported in previous machining research [21-27]. These models are reformulated here in a compact form to support multi-objective optimization of machining allowance in rectangular pocket milling.

The total energy consumption during the pocket milling process is expressed as the sum of the energy associated with feed motions and material removal,

$$E_{total} = P_f\, t_f + P_c\, t_c \qquad (1)$$

where P_f denotes the equivalent power consumed during non-cutting feed motions, including idle, spindle rotation, and feed drive power, and P_c is the cutting power required for chip formation. The variables t_f and t_c represent the feed time and cutting time, respectively. The cutting power is modeled as a function of the primary cutting parameters using a generalized empirical relationship,

$$P_c = C_P\, n_m^{\alpha}\, f_{vm}^{\beta}\, a_{pm}^{\gamma}\, a_{em}^{\delta} \qquad (2)$$

where n_m is the spindle speed, f_{vm} is the feed rate, a_{pm} and a_{em} are the axial and radial depths of cut, and $C_P, \alpha, \beta, \gamma,$ and δ are material- and machine-dependent coefficients.

The total machining time is decomposed into feed time and cutting time,

$$T_{total} = t_f + t_c \qquad (3)$$

For pocket milling, the feed time is estimated from the total tool travel length L_T and the feed rate,

$$t_f = \frac{L_T}{f_{vm}} \qquad (4)$$

while the cutting time is determined from the ratio of the removed material volume V to the material removal rate (MRR),

$$t_c = \frac{V}{MRR} \quad and\ MRR = \frac{v_m\, f_m\, a_{pm}\, a_{em}}{D_T} \qquad (5)$$

where v_m is the cutting speed and D_T is the tool diameter. Through these relations, the machining allowance directly influences both feed and cutting times by governing the number of passes and the total material volume removed.

The characteristic peripheral cutting force is incorporated using a compact analytical expression suitable for optimization [5, 14],

ISSN: 2594-1925

$$F_o = K_{tc}\, A_{em}\, h_{avg} \tag{6}$$

where $K_{tc}$is the tangential cutting force coefficient, $A_{em}$is the effective radial depth of cut, and $h_{avg}$is the average uncut chip thickness, which depends on the feed rate and machining allowance. This formulation allows cutting force to be evaluated efficiently without repeating detailed force derivations.

Based on the above models, the pocket milling process is formulated as a multi-objective optimization problem aiming to simultaneously minimize total energy consumption, total machining time, and characteristic cutting force,$min\ \{\ F_o\}$.

The decision variable vector is defined as $X = [d_h,\ a_{em},\ N_M,\ f_{vm1},\ f_{vm2}]$, where $d_h$represents the machining allowance distribution between rough and finish stages, $a_{em}$is the radial depth of cut, $N_M$is the spindle speed, and $f_{vm1}$and $f_{vm2}$are the feed rates in rough and finish milling, respectively. Practical machine-tool and process constraints are imposed to ensure feasibility. The resulting non-convex multi-objective optimization problem is solved using the NSGA-II algorithm to obtain a set of Pareto-optimal solutions.

2.2. Optimization Model for Pocket Milling

This section presents a simulation-based optimization framework for a two-stage pocket milling process consisting of rough and finish machining. The proposed model aims to simultaneously optimize three mutually conflicting performance objectives: total energy consumption (E_{total}), total machining time (T_{total}), and total characteristic peripheral cutting force $\left(F_{o,total}\right)$.

These objectives exhibit pronounced trade-off relationships. In general, reducing machining time leads to increased energy consumption and higher cutting forces, whereas minimizing cutting forces requires conservative cutting parameters that significantly prolong machining time. Similarly, reducing energy consumption often necessitates smaller cutting steps, which lowers productivity. Consequently, the problem is formulated as a non-convex multi-objective optimization problem that cannot be effectively solved using classical gradient-based or linear programming methods. To address this challenge, the Non-dominated Sorting Genetic Algorithm II (NSGA-II) is adopted to identify Pareto-optimal solutions [28-32].

The optimization problem involves five decision variables: the machining allowance distribution parameter between rough and finish stages (d_h), the effective radial depth of cut (a_{em}), the spindle speed (N_M), the feed rate in rough milling (f_{vm1}), and the feed rate in finish milling (f_{vm2}). The bounds of these variables are defined according to machine tool capabilities and tool limitations. To reflect practical operating conditions of the GSM-800 CNC milling machine, the spindle speed and feed rates are discretized to multiples of 10 rpm and 10 mm·min^{-1}, respectively.

In this study, the NSGA-II algorithm was implemented using a population size of 100 individuals and 200 generations. Tournament selection was used to select parent solutions, while simulated binary crossover and polynomial mutation were applied to generate offspring. The crossover probability and mutation probability were set to 0.90 and 0.10, respectively. The optimization process was terminated when the maximum number of generations was reached. These parameters were selected to maintain sufficient solution diversity and convergence stability while keeping the computational cost reasonable for the present machining optimization problem.

ISSN: 2594-1925

To ensure feasibility and industrial relevance, several technical constraints are imposed. The ratio between the feed rates of the rough and finish milling stages is constrained to maintain machining stability,

$$1.2 \leq \frac{f_{vm1}}{f_{vm2}} \leq 2 \quad (7)$$

ensuring that rough milling is performed at a higher feed rate without inducing excessive tool loading. In addition, the feed rate is constrained by the spindle speed through the kinematic relationship.

$$f_{vm} = n_m z f \quad (8)$$

where $n_m$is the spindle speed, $z$is the number of cutter teeth, and $f$is the feed per tooth. For a 10-mm end mill with four cutting edges machining polymer material, stable cutting conditions are experimentally observed when

$$0.05\, N_M \leq f_{vm} \leq 0.20\, N_M \quad (9)$$

These constraints effectively reduce vibration, prevent tool overload, and eliminate infeasible solutions during the optimization process.

The first optimization objective is total energy consumption. As coolant is not required for polymer machining, the total energy is expressed as the sum of idle, spindle rotation, feed drive, and cutting energies and is computed as

$$E = P_f T_f + P_c T_c \quad (10)$$

The second objective is total machining time, defined as the sum of feed time and cutting time, both of which depend on pocket geometry, machining allowance distribution, feed rates, spindle speed, and cutting depths.

The third objective is the characteristic peripheral cutting force. For optimization purposes, the cutting force is incorporated using a compact analytical expression,

$$F_o = K_{tc}\, A_{em}\, h_{avg} \quad (11)$$

where $K_{tc}$is the tangential cutting force coefficient, $A_{em}$is the effective radial depth of cut, and $h_{avg}$is the average uncut chip thickness, which depends on the feed rate and machining allowance. This formulation enables the cutting force to be directly evaluated within the optimization framework without repeating the detailed force derivation. Among the decision variables, the radial depth of cut and feed rate have the strongest influence on $F_o$and therefore dominate the force-related trade-offs in the optimization process.

The decision variables are encoded as a real-valued vector $X = [d_h, a_{em}, N_M, f_{vm1}, f_{vm2}]$ At each generation, NSGA-II applies non-dominated sorting and crowding-distance evaluation to preserve solution diversity while promoting convergence toward the Pareto-optimal front. To ensure comparability among objectives with different magnitudes, all objective functions are normalized using min–max normalization,

$$f_i'(X) = \frac{f_i(X) - min\,(f_i(X))}{max\,(f_i(X)) - min\,(f_i(X))} \quad (12)$$

ISSN: 2594-1925

The final optimization problem is formulated to minimize the normalized energy consumption, machining time, and cutting force subject to the defined technical constraints.

After obtaining the Pareto-optimal front, three representative solutions were selected for experimental comparison: the CAM-recommended baseline, the balanced Pareto-optimal solution, and the minimum-energy Pareto solution. The balanced Pareto-optimal solution was selected using the minimum normalized Euclidean distance to the ideal point. In this method, the ideal point corresponds to the individual minimum values of the normalized energy consumption, machining time, and cutting force. Therefore, the selected balanced solution represents a compromise among the three objectives, rather than the optimum of a single objective only.

2.3. Experimental setup for pocket milling

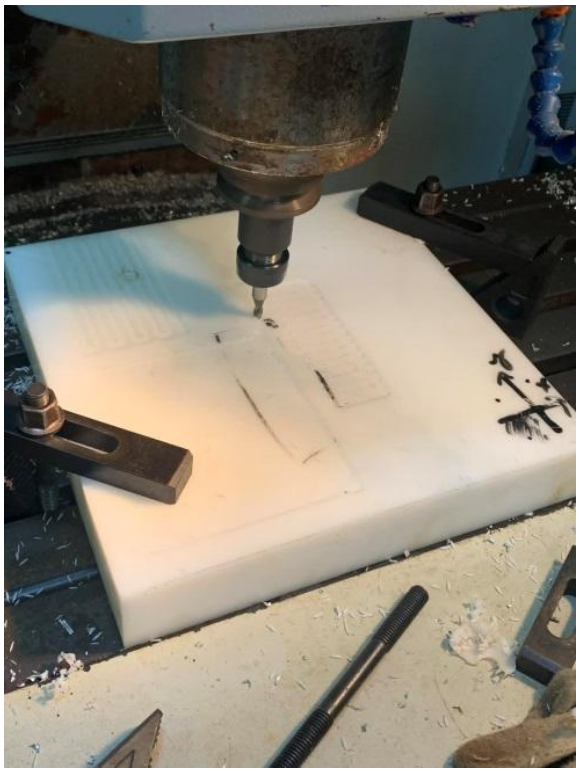

Figure 3. Experimental setup for pocket milling on a polymer workpiece using a CNC milling machine.

To validate the proposed energy–time–force models and the multi-objective optimization framework, a series of milling experiments were conducted on a CNC milling machine under controlled conditions. The experiments were designed to replicate the two-stage pocket milling process (rough and finish milling) assumed in the analytical and optimization models.

The experimental setup consisted of a three-axis CNC milling machine equipped with a vertical spindle, as shown in Figure 3. A polymer workpiece was rigidly clamped on the machine table using a mechanical fixture to ensure stable positioning during machining. A flat end mill with a diameter of 10 mm was employed for all experiments. The tool geometry and cutting parameters were selected in accordance with the ranges defined in the optimization model to ensure consistency between simulation and experimental validation.

Pocket milling was performed in two consecutive stages. In the first stage, rough milling was applied to remove the majority of the material using relatively higher feed rates and larger radial depths of cut. In the second stage, finish milling was carried out with reduced feed rates and cutting widths to

ISSN: 2594-1925

improve dimensional accuracy and surface quality. The machining allowance distribution between the two stages followed the values defined by the decision variable d_h.

Machining time was recorded from the CNC machining cycle for each pocket. Energy consumption was measured from the electrical energy used during the corresponding machining cycle, including spindle rotation, feed motion, and cutting. The peripheral cutting force was obtained using the force measurement system during the milling tests, and the characteristic maximum force value was used for comparison among the different machining strategies. After machining, the pocket depth was measured at representative positions using a depth gauge. The surface condition was evaluated through visual inspection of tool marks, wall uniformity, and bottom-surface quality. These measurement procedures provided a consistent basis for comparing the CAM-recommended baseline, the balanced Pareto-optimal solution, and the minimum-energy Pareto solution.

3. Results and discussion

At the beginning of the experimental validation, the pocket milling strategies corresponding to the baseline and Pareto-optimal solutions were implemented in a commercial CAM environment. Figure 4 illustrates the machining setup and toolpath generation in Autodesk Fusion, where three rectangular pockets were programmed on the same polymer workpiece using different parameter sets. Each pocket corresponds to a distinct machining strategy—namely the CAM-recommended baseline, the balanced Pareto-optimal solution, and the minimum-energy Pareto solution—allowing a direct and fair comparison under identical geometric and fixturing conditions. The visualization confirms consistent tool orientation, pocket geometry, and machining sequence, thereby ensuring that the observed differences in machining time, energy consumption, cutting force, and surface quality arise solely from the selected cutting parameters and machining allowance distributions.

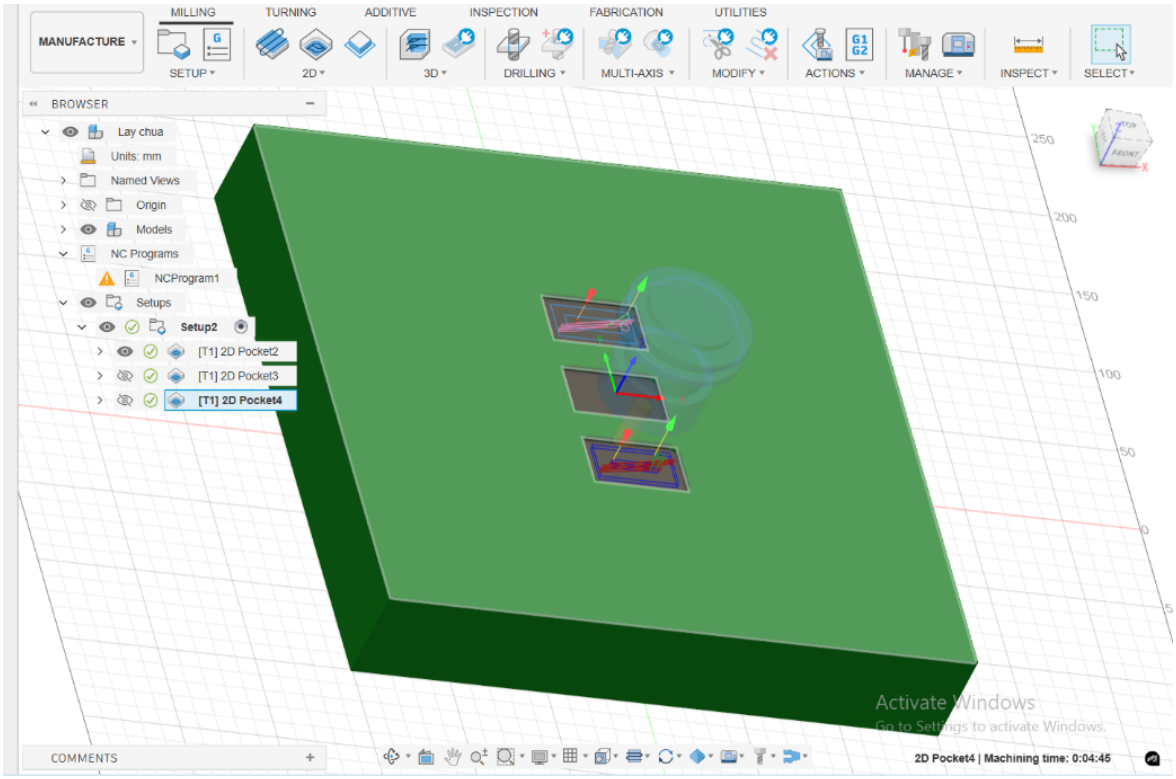

Figure 4. CAM implementation of rectangular pocket milling strategies in CAD software.

ISSN: 2594-1925

The proposed optimization framework was experimentally evaluated through three rectangular pocket milling trials conducted on polymer workpieces (workpiece size: 300 × 300 × 50 mm; pocket geometry: 50 × 30 × 20 mm). The three trials correspond to (i) a conventional baseline strategy using CAM-recommended parameters, (ii) a Pareto-optimal solution representing a balanced trade-off among energy, time, and cutting force, and (iii) an extreme Pareto solution targeting minimum energy consumption. Representative cavity geometries obtained under these three conditions are shown in Figure 5,6,7.

Figure 5. CAM-recommended baseline (smooth surface, long time, over-cut).

Using the cutting parameters automatically recommended by Autodesk Fusion, the first cavity (Figure 5) was machined at a spindle speed of 2000 rpm with a step-over of 6 mm and a programmed depth of −20 mm. Under these conditions, the machining time was 5 min 58.52 s, the measured peripheral cutting force was approximately 698.18 N, and the energy consumption was about 0.44 kWh. This strategy produced the smoothest surface finish among the three cases, as evidenced by the visually uniform cavity walls and bottom in Figure 5. However, the measured pocket depth reached approximately 24 mm, indicating an over-machining error of nearly 2 mm relative to the target depth. This depth deviation may be attributed to the CAM-default allowance setting, accumulated depth-control error during multi-pass machining, and the difference between the programmed toolpath depth and the actual material removal obtained on the polymer workpiece. Although the conservative CAM-recommended parameters ensured good surface quality and stable cutting behavior, the excessive machining time and significant dimensional deviation limit their suitability for precision pocket milling applications.

ISSN: 2594-1925

Figure 6. Balanced Pareto-optimal solution (shortest time, lowest force, poor surface).

The second cavity (Figure 6) was machined using a parameter set selected from the Pareto front as the most balanced solution, with a spindle speed of 5000 rpm, a reduced step-over of 4.7301 mm, and a programmed depth of −17.9927 mm. This configuration reduced the machining time to 2 min 26.47 s, corresponding to approximately 41% of the baseline machining time. At the same time, the peripheral cutting force decreased to 382.73 N, which is about 55% of that observed in the CAM-recommended case, while energy consumption increased slightly to 0.52 kWh. As shown in Figure 6, visible tool marks appear on the cavity surface, indicating degraded surface quality compared with the baseline. Nevertheless, the measured pocket depth was approximately 22 mm, closely matching the desired geometry and eliminating the over-cut observed in the first case. This result demonstrates that the optimized machining allowance distribution effectively improves dimensional accuracy and productivity, albeit at the expense of surface finish.

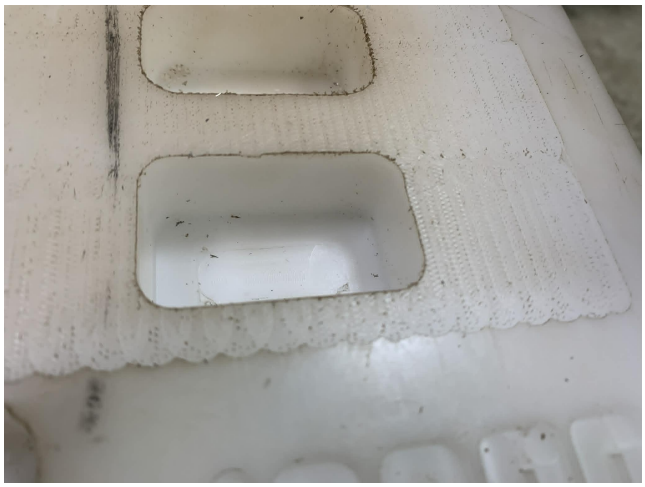

Figure 7. Minimum-energy Pareto-optimal solution.

The third cavity (Figure 7) corresponds to the Pareto solution that minimizes energy consumption. This cavity was machined at 5000 rpm with a large step-over of 9.9945 mm and a programmed depth of −17.996 mm. The measured energy consumption was the lowest among all trials, approximately 0.267 kWh, confirming the effectiveness of the energy-oriented optimization objective. However, the machining time remained relatively long at 5 min 47.48 s, only marginally shorter than the CAM-recommended case, while the peripheral cutting force increased substantially to approximately 1203.45 N, representing nearly 1.7 times the baseline force and more than three times that of the

ISSN: 2594-1925

balanced solution. As illustrated in Figure 10(c), the cavity exhibits a relatively smooth overall appearance with less pronounced tool-path marks than in Figure 10(b), but the bottom surface remains uneven. Although no chatter or tool jamming was observed, the high cutting force implies increased mechanical loading, which may negatively affect tool life and machine reliability in long-term operation.

A comparative analysis of the three cavities shown in Figure 5-7 clearly reveals the trade-off structure predicted by the multi-objective optimization model. The CAM-recommended strategy (Figure 5) prioritizes surface quality and conservative cutting but results in long machining time and unacceptable depth deviation. The minimum-energy strategy (Figure 7) achieves the lowest energy consumption but introduces excessive cutting force with only marginal improvement in machining time. In contrast, the balanced Pareto-optimal solution (Figure 6) provides the most practically relevant compromise, achieving significant reductions in machining time and cutting force while maintaining acceptable dimensional accuracy. These results confirm that the proposed optimization framework enables informed selection of machining parameters based on specific production priorities, rather than relying solely on default CAM-generated settings.

4. Conclusion

This study presented an analytical and multi-objective optimization framework for determining an efficient machining allowance in rectangular pocket milling. By explicitly incorporating machining allowance into energy, time, and cutting force models, the proposed approach enables a quantitative evaluation of trade-offs in two-stage rough–finish milling processes.

Experimental validation on polymer workpieces demonstrated the practical potential of the proposed optimization framework under the tested conditions. Compared with CAM-recommended parameters, the balanced Pareto-optimal solution reduced machining time from 5 min 58.52 s to 2 min 26.47 s, corresponding to an approximate 59% reduction in machining time, while simultaneously decreasing the peripheral cutting force from 698.18 N to 382.73 N, corresponding to an approximate 45% reduction. In addition, the optimized strategy reduced the over-machining error observed in the CAM-based approach and achieved a pocket depth closer to the target geometry. These results indicate that machining allowance optimization can contribute to improved efficiency and dimensional control in rectangular pocket milling.

The minimum-energy Pareto solution achieved the lowest energy consumption, decreasing from 0.44 kWh for the CAM baseline to 0.267 kWh. However, this benefit was accompanied by a substantial increase in cutting force to 1203.45 N, highlighting the mechanical risks associated with single-objective energy minimization. This finding underscores the necessity of multi-objective optimization, as extreme solutions may compromise tool life, dimensional stability, and machine reliability despite energy savings.

Overall, the proposed framework provides a rational and quantitative method for selecting machining allowance and cutting parameters based on explicit performance targets. Rather than relying only on default CAM recommendations, process planners may use Pareto-optimal solutions to balance productivity, energy efficiency, cutting force, and dimensional accuracy according to specific machining requirements. However, the present validation was limited to polymer workpieces and a limited number of experimental trials. Future work should extend the method to metallic materials, additional pocket geometries, repeated experiments, and quantitative surface roughness measurements to further evaluate the robustness and general applicability of the proposed approach.

ISSN: 2594-1925

5. Authorship acknowledgments

Tran Thanh Tung: Conceptualization; Methodology; Investigation; Data Analysis; Writing – Original Draft. *Nguyen Thi Anh:* Formal Analysis; Investigation; Data Analysis. *Nguyen Xuan Quynh:* Resources; Data Analysis. *Tran Vu Minh:* Conceptualization; Validation; Writing – Review and Editing.

References

[1] A. De Bartolomeis, D. A. Axinte, S. J. Pickering, and L. Zhou, "Future research directions in the machining of Inconel 718," *Journal of Materials Processing Technology*, vol. 297, p. 117260, 2021, doi: 10.1016/j.jmatprotec.2021.117260.
[2] N. T. Anh, N. X. Quynh, and T. T. Tung, "A Milling Technique for the Fabrication of Mechanical Parts with Thin-Walled Ribs," *Eng. Technol. Sci. Res.*, vol. 15, no. 4, pp. 24815–24819, Aug. 2025, doi: 10.48084/etasr.11136.
[3] M. Soori, M. Asmael, and D. Solyalı, "Sustainable CNC machining operations, a review," *Sustainable Operations and Computers*, vol. 5, pp. 73–87, 2024, doi: 10.1016/j.susoc.2024.01.001.
[4] M. Hourmand, A. A. D. Sarhan, and M. Sayuti, "A Comprehensive Review on Machining of Titanium Alloys," *Arab J Sci Eng*, vol. 46, pp. 7087–7123, 2021, doi: 10.1007/s13369-021-05420-1.
[5] N. T. Anh and T. T. Tung, "Development and validation of finite element model of milling thin-walled part," *Applications in Engineering Science*, vol. 25, p. 100285, 2026, doi: 10.1016/j.apples.2025.100285.
[6] G. Wang, W. -L. Li, C. Jiang, and H. Ding, "Machining Allowance Calculation for Robotic Edge Milling an Aircraft Skin Considering the Deformation of Assembly Process," *IEEE/ASME Transactions on Mechatronics*, vol. 27, no. 5, pp. 3350–3361, Oct. 2022, doi: 10.1109/TMECH.2021.3131309.
[7] B. Wu, Y. Zhang, G. Liu, and Z. Wang, "Feedrate optimization method based on machining allowance optimization and constant power constraint," *Int J Adv Manuf Technol*, vol. 115, pp. 3345–3360, 2021, doi: 10.1007/s00170-021-07381-z.
[8] M. Belhadj, R. Kromer, S. Werda, S. Leleu, and A. El Mansori, "Effect of cold metal transfer-based wire arc additive manufacturing parameters on geometry and machining allowance," *Int J Adv Manuf Technol*, vol. 131, pp. 739–748, 2024, doi: 10.1007/s00170-023-11835-x.
[9] B. Burhanudin, M. Margono, E. Suryono, N. T. Atmoko, and Z. Zainuddin, "The Effect of Finishing Allowance and Milling Methode on Surface Roughness in the Finishing Process of Al5052 and Al7075," *KEM*, vol. 935, pp. 63–71, Nov. 2022, doi: 10.4028/p-yt2516.
[10] I. Daniyan, K. Mpofu, and F. Fameso, "Computer-aided modelling and experimental evaluation of the pocket milling operation for alloy tool steel (AISI D3)," *Int J Adv Manuf Technol*, vol. 122, pp. 4453–4466, 2022, doi: 10.1007/s00170-022-09979-3.
[11] R. Mellacheruvu and M. Venkateswara Rao, "Application of artificial neural networks and genetic algorithm for optimizing process parameters in pocket milling of AA7075," *Journal of Scientific & Industrial Research*, vol. 81, no. 9, pp. 911–921, 2022, doi: 10.56042/jsir.v81i09.55874.
[12] Z. Chen, C. H. E. N., X. C. H. E. N., and Y. L. I. U., "Framework and development of data-driven physics based model with application in dimensional accuracy prediction in pocket milling," *Chinese Journal of Aeronautics*, vol. 34, no. 6, pp. 162–177, 2021, doi: 10.1016/j.cja.2020.09.011.
[13] Z. Duan, C. Li, W. Ding, Y. Ning, and M. Yang, "Milling Force Model for Aviation Aluminum Alloy: Academic Insight and Perspective Analysis," *Chin. J. Mech. Eng.*, vol. 34, no. 1, p. 18, 2021, doi: 10.1186/s10033-021-00536-9.
[14] N. T. Anh and T. T. Tung, "Cutting force prediction in end milling processes: Analytical models and applications," *Applications in Engineering Science*, vol. 23, p. 100250, 2025, doi: 10.1016/j.apples.2025.100250.
[15] B. Yan, B. Wang, L. Zhu, C. Zhang, P. Wang, and G. Zhao, "Towards high milling accuracy of

ISSN: 2594-1925

turbine blades: A review," *Mechanical Systems and Signal Processing*, vol. 170, p. 108727, 2022, doi: 10.1016/j.ymssp.2021.108727.
[16] J. H. Navarro-Devia, Y. Chen, and D. V. Dao, "Chatter detection in milling processes—a review on signal processing and condition classification," *Int J Adv Manuf Technol*, vol. 125, pp. 3943–3980, 2023, doi: 10.1007/s00170-023-10969-2.
[17] M. S. El-Eskandarany, A. Al-Hazza, L. A. Al-Hajji, N. Ali, A. A. Al-Duweesh, M. Banyan, and F. Al-Ajmi, "Mechanical Milling: A Superior Nanotechnological Tool for Fabrication of Nanocrystalline and Nanocomposite Materials," *Nanomaterials*, vol. 11, no. 10, p. 2484, 2021, doi: 10.3390/nano11102484.
[18] Rahul A. Mali, T. V. K. Gupta, and J. Ramkumar, "A comprehensive review of free-form surface milling—Advances over a decade," *Journal of Manufacturing Processes*, vol. 62, pp. 132–167, 2021, doi: 10.1016/j.jmapro.2020.12.014.
[19] Z. H. A. O. Guolong, "Cutting force model and damage formation mechanism in milling of 70wt% Si/Al composite," *Chinese Journal of Aeronautics*, vol. 36, no. 7, pp. 114–128, 2023, doi: 10.1016/j.cja.2022.07.018.
[20] José David Pérez-Ruiz, "On the relationship between cutting forces and anisotropy features in the milling of LPBF Inconel 718 for near net shape parts," *International Journal of Machine Tools and Manufacture*, vol. 170, p. 103801, 2021, doi: 10.1016/j.ijmachtools.2021.103801.
[21] Markus Brillinger, "Energy prediction for CNC machining with machine learning," *CIRP Journal of Manufacturing Science and Technology*, vol. 35, pp. 715–723, 2021, doi: 10.1016/j.cirpj.2021.07.014.
[22] Yuying Yang, "Mechanical performance of 316 L stainless steel by hybrid directed energy deposition and thermal milling process," *Journal of Materials Processing Technology*, vol. 291, p. 117023, 2021, doi: 10.1016/j.jmatprotec.2020.117023.
[23] Vincent Aizebeoje Balogun and Paul Tarisai Mativenga, "Modelling of direct energy requirements in mechanical machining processes," *Journal of Cleaner Production*, vol. 41, pp. 179–186, 2013, doi: 10.1016/j.jclepro.2012.10.015.
[24] K. He, H. Hong, R. Tang, and J. Wei, "Analysis of Multi-Objective Optimization of Machining Allowance Distribution and Parameters for Energy Saving Strategy," *Sustainability*, vol. 12, no. 16, p. 638, 2020, doi: 10.3390/su12060638.
[25] A. Pajaziti, O. Tafilaj, A. Gjelaj, and B. Berisha, "Optimization of Toolpath Planning and CNC Machine Performance in Time-Efficient Machining," *Machines*, vol. 13, no. 1, p. 65, 2025, doi: 10.3390/machines13010065.
[26] R. Saravanan and V. Janakiraman, "Study on Reduction of Machining Time in CNC Turning Centre by Genetic Algorithm," in *International Conference on Computational Intelligence and Multimedia Applications (ICCIMA 2007)*, Sivakasi, India, 2007, pp. 481–486, doi: 10.1109/ICCIMA.2007.92.
[27] K. He, R. Tang, Z. Zhang, and W. Sun, "Energy Consumption Prediction System of Mechanical Processes Based on Empirical Models and Computer-Aided Manufacturing," *ASME J. Comput. Inf. Sci. Eng.*, vol. 16, no. 4, p. 041008, Dec. 2016, doi: 10.1115/1.4033921.
[28] Wu Deng, "An enhanced fast non-dominated solution sorting genetic algorithm for multi-objective problems," *Information Sciences*, vol. 585, pp. 441–453, 2022, doi: 10.1016/j.ins.2021.11.052.
[29] W. Zheng and B. Doerr, "Approximation Guarantees for the Nondominated Sorting Genetic Algorithm II (NSGA-II)," *IEEE Transactions on Evolutionary Computation*, vol. 29, no. 4, pp. 891–905, Aug. 2025, doi: 10.1109/TEVC.2024.3402996.
[30] M. Babor, L. Pedersen, U. Kidmose, O. Paquet-Durand, and B. Hitzmann, "Application of Non-Dominated Sorting Genetic Algorithm (NSGA-II) to Increase the Efficiency of Bakery Production: A Case Study," *Processes*, vol. 10, no. 8, p. 1623, 2022, doi: 10.3390/pr10081623.
[31] M. Moshref, R. Al-Sayyed, and S. Al-Sharaeh, "An Enhanced Multi-Objective Non-Dominated

ISSN: 2594-1925

Sorting Genetic Routing Algorithm for Improving the QoS in Wireless Sensor Networks," *IEEE Access*, vol. 9, pp. 149176–149195, 2021, doi: 10.1109/ACCESS.2021.3122526.
[32] Y. -C. Chang, K. -H. Chang, and C. -P. Zheng, "Application of a Non-Dominated Sorting Genetic Algorithm to Solve a Bi-Objective Scheduling Problem Regarding Printed Circuit Boards," *Mathematics*, vol. 10, no. 12, p. 2305, 2022, doi: 10.3390/math10122305.

ISSN: 2594-1925